Hindawi
Shock and Vibration
Volume 2020, Article ID 8214021, 8 pages
https://doi.org/10.1155/2020/8214021

Research Article

Study of the Growth Process of Original Crack in the Surrounding Rock of Tunnel under the Adjacent Explosive Load

Kang Liu, Dongming Guo, Xinchao Kang, and Jun Zhang

China University of Mining & Technology, No. 11 Xueyuan Road, Haidian District, Beijing, China

Correspondence should be addressed to Kang Liu; liukang0512@163.com

Received 6 August 2019; Accepted 21 November 2019; Published 8 January 2020

Academic Editor: Angelo Marcelo Tusset

The surrounding rock damage of a tunnel under adjacent explosive load is often manifested as the growth of the original crack. In order to thoroughly understand the crack growth mechanism, in this study, the growth process of the original crack was investigated in detail by the dynamic caustics experiment. The experimental study shows that the growth of original crack is the result of the combined action of explosion stress wave and explosive gas. The quasi-static stress generated by the explosive gas was superimposed on the weakened stress field, resulting in the formation of the peak of the main stress difference in the surrounding rock, moving towards the adjacent tunnel in the form of an arc wave. With the arc wave moving towards the original crack, the growth rate of the original crack increases rapidly. During the period of 200 μs to 250 μs, the crack growth rate oscillates at the peak, and its size is approximately equal to the moving speed of the arc wave. Based on the experimental results and microscopic damage mechanics, the high stress concentration at the original crack tip under the stress wave first causes damage localization and the weakest chain is formed by the penetration of the damage localization zones by microcracks by special distribution law. Subsequently, the original crack starts to initiate and grow along the direction of the weakest chain.

1. Introduction

In recent years, with rapid improvement of mechanization, the roadheader gradually replaces the drilling and blasting method and is applied to the excavation of the tunnel. However, for the construction of rigid mountain tunnels and coal mine rock tunnels, the roadheader consumes high energy and has low efficiency and high failure rate. Therefore, the drilling and blasting method is still widely used. However, in addition to completing the necessary crushing work, the explosive load also causes unavoidable damage to the adjacent tunnel. Therefore, studying the dynamic response of adjacent tunnels under the explosive load to ensure the safety of the existing tunnel is important [1].

In view of the dynamic response of the adjacent tunnel under explosive load, detailed investigation has been carried out through theoretical analysis, field test, and numerical analysis. In terms of theoretical analysis, the dynamic response problem of the adjacent tunnel under explosive load is generally simplified to the dynamic stress concentration around the hole under stress wave. Stress and displacement expressions about the lining and the surrounding rock of the adjacent tunnel under elastic wave were derived by the wave theory [2]. In addition, Li et al. [3] reported the distribution law of the dynamic stress concentration coefficient around the surrounding rock of the adjacent tunnel under explosive load. In the field test and numerical analysis, based on the stress field or particle vibration velocity of the surrounding rock, the dynamic response of the surrounding rock of the adjacent tunnel under explosive load has been studied. Explosive excavation easily damages the surrounding rock of the adjacent tunnels, such as rock cracks or roof rock spalling. Rock damage is related to dynamic mechanical characteristics and explosive vibration characteristics of surrounding rock [4]. The maximum particle vibration velocity and maximum tensile stress are located at the tunnel vault and the side wall corner [5]. In addition, the degree of damage of the surrounding rock of the adjacent tunnel gradually increases with increasing peak particle velocity (PPV) [6]. Therefore, controlling the PPV could ensure the

safety of adjacent tunnels. Moreover, the judging criterion is proposed based on the PPV and the maximum tensile stress in order to ensure the safety and stability of the adjacent tunnels under the explosive load [7]. The above studies generally assume that the surrounding rock is intact and mainly analyzed the surrounding rock stress field and vibration velocity field of the adjacent tunnel under the explosive load to obtain the main disturbance areas about the surrounding rock of the adjacent tunnel.

Generally, many cracks and other defects exist in the surrounding rock of the tunnel. Crack growth under the explosive load often becomes the main manifestation of the surrounding rock failure of the tunnel [8]. The face-blasting side of the tunnel is believed as the main disturbance zone under the adjacent explosive load. However, many model experiments have shown that the back-blasting side also tends to be the main disturbance zone and appears as the growth of the original crack in the presence of original cracks in the back-blasting side [9]. Therefore, the objective of this study was to investigate the original crack in the back-blasting side of the surrounding rock, which is often neglected. The transient property of crack growth makes the study difficult, and the dynamic caustic method is one of the most effective research methods at present. Through the matching dynamic caustic experimental system, the whole growth process of crack can be clearly captured, which lays a foundation for the study of dynamic crack growth law and mechanism. For example, the relationship between the dynamic stress intensity factor, the crack growth velocity, and the acceleration of a brittle material under explosive load by dynamic caustic experiment has been investigated [10]. The dynamic caustic experiments also found that stress concentration resulting from the compressive stress pulses at the bottom of the notch did not create a crack propagation phenomenon. The tensile stress pulses played an important role in the incubation, nucleation, and propagation of cracks from the bottom of notches in thin strips [11, 12].

Currently, the dynamic caustic method had been primarily applied to study the crack growth law and growth mechanism of the surrounding rock in the adjacent tunnel under explosive load, indicating that the final growth displacement of the original crack is related to the fluctuation time of the dynamic stress intensity factor around the peak [13].

In view of the superiority of the dynamic caustic method, in this study, the crack growth process of the surrounding rock in the adjacent tunnel under explosive load was investigated by this method.

2. Methods and Materials

2.1. Experimental Method and Principle. The paper adopts the dynamic caustics method to study. The principle of the method is as follows. The explosive load consists of the actions of the stress wave and the quasi-static stress of the explosive gas. When the explosive load acts on the test piece containing the crack defect, the tensile stress and shear stress generate on the free surface of the crack, and thus, the stress concentration is generated on the crack tip. As a result, the elastoplastic deformation occurs at the tip with the change in thickness, changing the refractive index of this area accordingly. When a beam of uniform and stable parallel light is irradiated into the region, the refraction of the light causes deviation of the emergent light with the original direction. When placing a nontransparent sheet at the reference plane position, the obvious dark area, called focal speckle, is observed. The above method transforms this problem from dynamic stress concentration of the crack tip to the geometric shadow optical pattern and simplifies the analysis of this problem. This method is called the dynamic caustics method [14]. Since the crack tip is subjected to the combined action of shear wave, compression wave, reflected tensile wave, and unloading wave, the crack appears as a composite growth. Figure 1 shows the image-forming principle of the focal speckle.

2.2. Experimental System. The dynamic caustics experimental system shown in Figure 2 includes a laser emitter for a stable point source, a beam expander for emitting a point source, two lenses for a stable light field, a fixed device for fixing the test piece, and a high-speed camera for the data acquisition.

Figure 2 shows that the distance between the beam expander and lens 1 has to be adjusted properly, so that the point source is expanded by the beam expander to form a stable light field filled with lens 1. After the stable light spreads through lens 1, the parallel light appears and shines on the test specimen. When the test specimen suffers from the explosive load, the crack tip generates stress concentration. Because of the refraction of light, the emergent light from the rear surface of the test specimen deflects. When placing a reference plane between the test specimen and lens 2, an obvious dark area, known as focal speckle, was observed. At this moment, the high-speed camera can capture the focal speckle through lens 2.

2.3. Test Data. Through the dynamic method, these data are acquired.

2.3.1. Crack Growth Rate. The high-speed camera can record a series of pictures of the crack growth process at set intervals. Measuring the distance from the geometric center of the focal speckle to the reference point successively, the length of the crack at different times can be determined. Adopting the Origin software, the curve of the crack growth velocity and time can be obtained, as expressed by the following equation:

$$v = \dot{l}(t). \tag{1}$$

2.3.2. Dynamic Stress Intensity Factor. The dynamic stress intensity factor (K) is positively correlated with the stress field at the crack tip and reflects the stress concentration degree at the crack tip. The dynamic stress intensity factor can be expressed as [15]

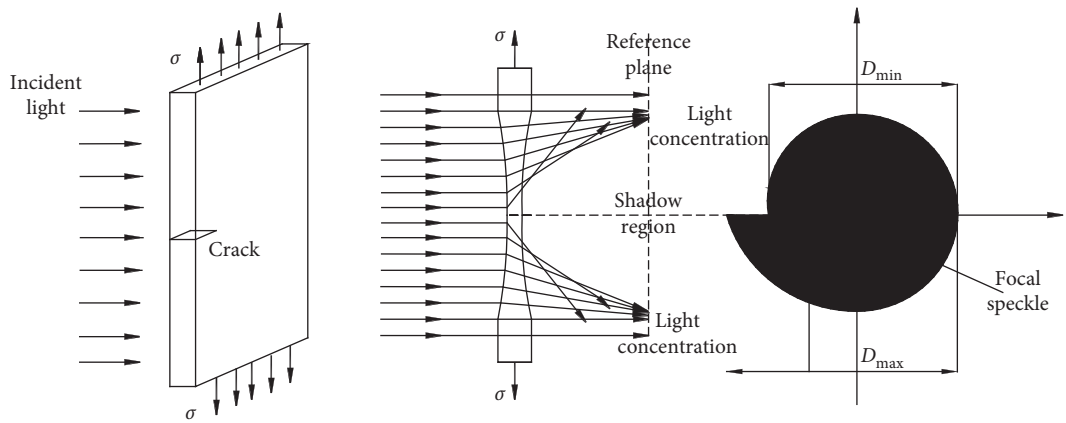

Figure 1: Schematic diagram of caustics formation.

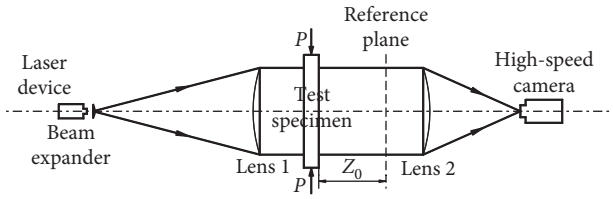

Figure 2: Schematic diagram of the transmission caustics experimental system.

$$\begin{cases} K_{\mathrm{I}} = \dfrac{2\sqrt{2\pi}}{3g^{5/2}z_0 Cd} D_{\max}^{5/2}, \\ K_{\Pi} = \mu K_{\mathrm{I}}, \end{cases} \tag{2}$$

where z_0 is the distance between the reference plain and specimen, c is the optical stress constant of plexiglass plate, d is the thickness of plexiglass panel, μ is the proportionality coefficient of dynamic stress intensity factor, which can be acquired through the $(D_{\max} - D_{\min})/D_{\max}$, and g is the numerical factor of the stress intensity, which can be determined by μ. The diameters $D_{\max}$ and $D_{\min}$ of the focal speckle were obtained through the series of pictures of the experimental system.

2.3.3. Dynamic Energy Release Rate. Dynamic energy release rate has great driving effects on the crack growth. Freund [16] finds that there is a correlation between the dynamic energy release rate (G) and the dynamic stress intensity factor, and through analysis, the relationship under the plane stress condition is expressed as

$$G = \frac{1}{E}\left[A_1(\nu)K_1^2 + A_{\Pi}(\nu)K_{\Pi}^2\right], \tag{3}$$

where E is the elastic modulus of the material and $A_1(\nu)$ and $A_{\Pi}(\nu)$ are the velocity function of crack growth.

When $\nu = 0$, $A_1(\nu) = A_{\Pi}(\nu) = 1$.

When $\nu \neq 0$, $A_1(\nu) = \nu^2\alpha_d/((1-\nu)c_s^2 D)$, $A_{\Pi}(\nu) = \nu^2\alpha_d/((1-\nu)c_s^2 D)$. Here, $\alpha_d = \sqrt{1-\nu^2/c_d^2}$, $\alpha_s = \sqrt{1-\nu^2/c_s^2}$, and $D = 4\alpha_d\alpha_s - (1+\alpha_s^2)^2$, where c_d is the expansion wave velocity and c_s is the shear wave velocity.

2.4. Experimental Material Selection and Experimental Model Dimensions. The physical and mechanical parameters of rock materials or artificial stones are close to those of the surrounding rock medium of the tunnel; therefore, these materials are more suitable as a model material. However, due to the brittleness of the rock materials, the processing of the model causes inevitable damage, and the rock material itself has some crack defects, increasing the dispersion of experimental results and thus achieving ideal experimental results is difficult. In addition, the similar model experiment can only obtain the crack growth path, but the dynamic evolution process of the crack, the kinematic parameters, and the dynamic parameters of the crack growth are not acquired. Therefore, to better simulate the disturbance process of the explosive load on the adjacent tunnel, a material with good plasticity and isotropic is used. In addition, the transmission-type caustic experiment system requires the experimental materials with higher transmittance. The polymethyl methacrylate (PMMA) has all these advantages and has been subjected to relevant investigation and experiments with a good experimental effect. Table 1 shows the dynamic optical constants of PMMA [17].

The experimental model size is $300 \times 300 \times 5\ \mathrm{mm}^3$, as shown in Figure 3. The straight-wall semicircular arch hole is processed through the middle of the plate to simulate the adjacent tunnel. The lower part of the hole is a semirectangular shape with a size of $40 \times 20\ \mathrm{mm}^2$, and the upper part is a semicircular arch with a radius of 20 mm. The length of the original crack on the back-blasting side of the tunnel is 5 mm. The blasthole, with a diameter of 6 mm, is processed on the left side of the hole and is filled with a single layer of lead azide explosive to simulate the drilling and blasting method construction of the adjacent tunnel.

3. Experimental Results and Discussion

3.1. Experimental Phenomenon Analysis. Figure 4 includes a series of focal speckle pictures that record the growth process of the original crack in the back-blasting side of the adjacent tunnel under explosive load. After the explosion, the shock wave quickly attenuates to the compression wave and propagates to the surroundings. The pictures from 30 μs to

Table 1: Dynamic optical constants of the model material.

Material	ρ (kg/m^3)	C_d (m/s)	C_s (m/s)	E_d (GN/m^2)	v_d	$\lvert C_t \rvert$ (m^2/N)
PMMA	1145	2190	1200	3.595	0.32	0.084

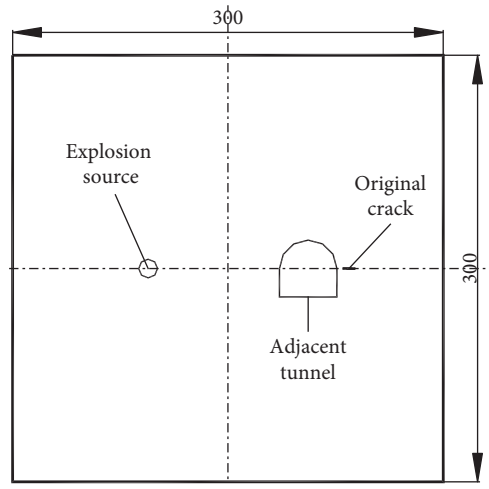

Figure 3: Schematic diagram of the experimental model.

50 μs show that the annular stress concentration zone is formed by the compression wave and gradually propagates to the back-blasting side. After 60 μs, the annular stress concentration zone disappears. When $t = 70\,\mu$s, the focal speckle appears at both the ends of the original crack in the back-blasting side of the adjacent tunnel. This phenomenon indicates that part of the stress wave energy diffracts to the back-blasting side and acts on the original crack, generating stress concentration at both the ends of original crack. The effect of stress wave is manifested in two aspects. The stress wave across the tip produces a shear stress along the crack tendency, and the stress wave reflected by the tip produces a reflection tensile force. However, the original crack does not grow at this time, indicating that the dynamic stress intensity factor at the crack tip has not yet reached dynamic fracture toughness. When $t = 90\,\mu$s, a large amount of explosive gas accumulated in the blasthole begins to release, because of the radial crack of the blasthole. At $t = 130\,\mu$s, the arc stress concentration zone is observed around the blasthole. When t is in the range 110–150 μs, the arc-shaped stress concentration zone gradually approaches the original crack in the back-blasting side of the tunnel. At this moment, the focal speckle of the original crack tip gradually increases, indicating that the arc-shaped stress concentration zone has a great promotion to the crack initiation. When $t = 170\,\mu$s, the crack starts to grow, and with the gradual approach of the arc-shaped stress concentration region, the original crack rapidly propagates. When $t = 310\,\mu$s, the arc-shaped stress concentration region catches up with the growing crack tip. After that, the diameter of the focal speckle continuously decreases, indicating that the driving force for the crack growth continues to diminish or disappear after the arc-shaped stress concentration region crosses the growing crack tip. Subsequently, the elastic energy stored in the surrounding rock is released, and unloading wave starts to play a leading role in the crack growth. Because of the radial tensile stress of the unloading wave, the growing crack warps downward. At last, in the final stage, with the consumption of the elastic energy, crack arrests.

After the explosion, the shock wave first acts on the surrounding rock to form the blasting cavity and the surrounding fissure zone. Subsequently, the explosive gas filled with the blasthole acts on the hole wall in the form of a pulse load and generates quasi-static stress in the surrounding rock. This observation is consistent with the above phenomenon. The crack growth in the back-blasting side of the adjacent tunnel is affected by the explosion compression wave (stress wave), the quasi-static stress of the explosive gas, and the unloading wave generated by the release of elastic energy. Although the compression wave cannot induce the crack in the back-blasting side to grow at the macro level with the propagation and diffraction of compression wave, it plays an important role in the damage process and energy accumulation before the crack initiation. The quasi-static stress of the explosive gas acts on the whole process of crack growth and plays a leading role in the early and middle stages of the crack growth. When the generated arc-shaped stress concentration region crosses the growing crack, the pushing effect on the crack growth is weakened or disappeared. The unloading wave mainly acts on the late stage of the crack growth, and the vertical stress generated causes the crack to warp and grow downward.

3.2. Kinematic Analysis of Crack Growth Process. The growth of the original crack in the back-blasting side of the surrounding rock of the adjacent tunnel is related to the arc-shaped stress concentration zone formed by the quasi-static stress. When the arc-shaped stress concentration area catches up and gradually approaches the growing crack, it increases the focal speckle diameter at the crack tip and the crack rapidly grows. The maximum growth rate of the crack occurs, when the relative distance between the arc-shaped stress concentration region and the growing crack tip is equal to 1 cm. At this time, the crack growth rate is approximately equal to the propagation velocity of the arc-shaped stress concentration region, as shown in Figure 5, indicating that when the stress concentration region crosses the growing crack, the diameter of the focal speckle at the crack tip gradually decreases, the crack growth rate gradually decreases, and the crack growth is finally terminated. Thus, the crack growth process can be divided into two stages. In the first stage, the arc-shaped stress concentration region catches up with the growing crack tip. In the second stage, the arc-shaped stress concentration region is away from the growing crack tip. Since the arc-shaped stress concentration region propagates in the form of waves, it is simply referred to as an arc wave, and the schematic diagram is shown in Figure 6.

Figure 6(a) shows a black spot (focal speckle) surrounded by a bright line at the tip of the growing crack, and an arc wave exists to the left of the focal speckle. These experiments confirmed that the arc wave has an important

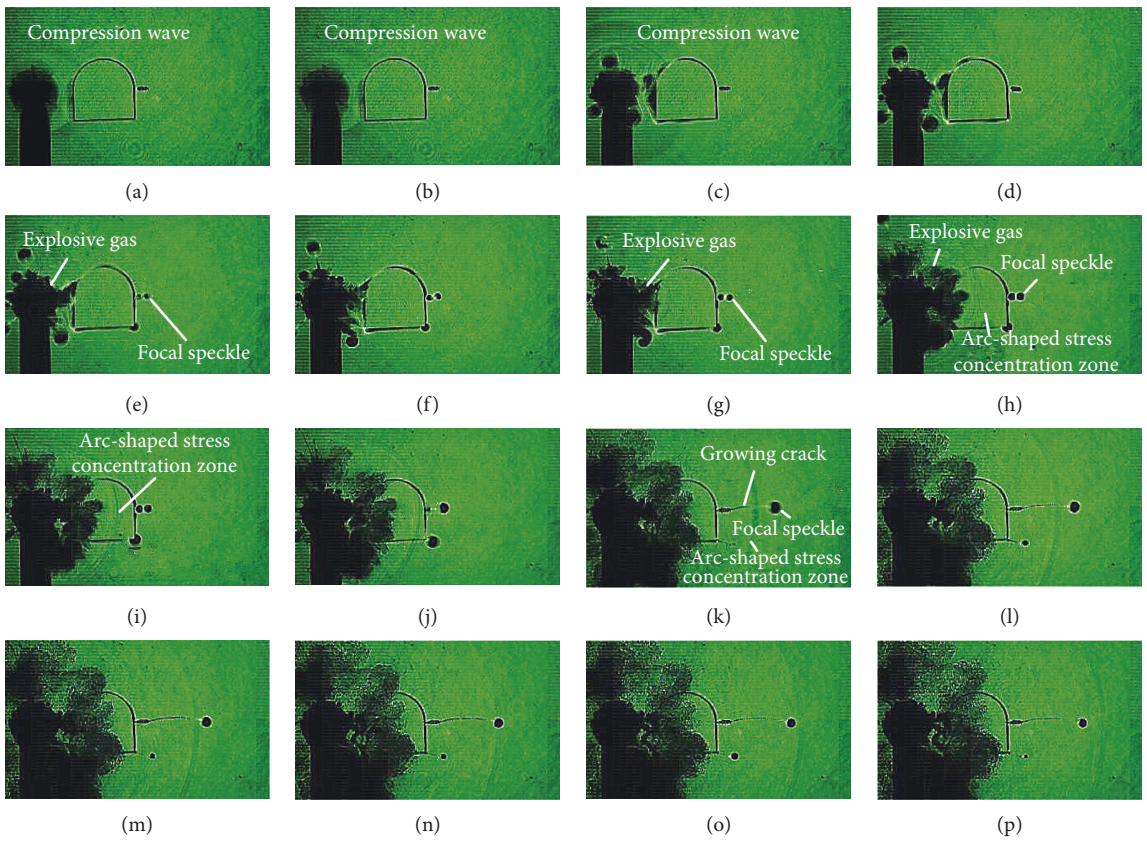

FIGURE 4: A series of caustics pictures of the explosion loads acting on the original crack of the adjacent tunnels. (a) $t = 30\,\mu s$, (b)$t = 40\,\mu s$, (c) $t = 50\,\mu s$, (d) $t = 60\,\mu s$, (e) $t = 70\,\mu s$, (f) $t = 80\,\mu s$, (g) $t = 90\,\mu s$, (h) $t = 130\,\mu s$, (i) $t = 150\,\mu s$, (j) $t = 170\,\mu s$, (k) $t = 250\,\mu s$, (l) $t = 270\,\mu s$, (m) $t = 290\,\mu s$, (n) $t = 310\,\mu s$, (o) $t = 330\,\mu s$, and (p) $t = 350\,\mu s$.

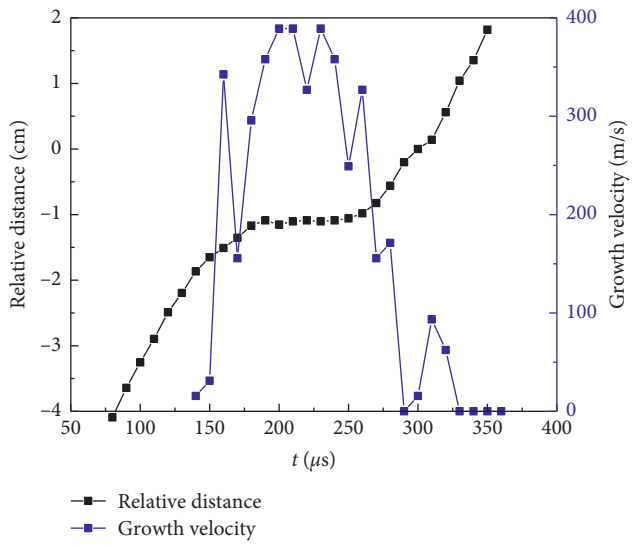

FIGURE 5: Velocity curve of the original crack growth and the relative displacement curves of the arc wave and the growing crack tip.

influence on the crack growth, and the average moving speed of the arc wave is 350 m/s, as shown in Figure 7. When the arc wave gradually approaches the tip of the growing crack, the crack growth rate increases significantly. When the arc wave crosses the focal speckle of the crack tip, the crack growth velocity gradually decreases to zero.

3.3. Energy Analysis of Crack Growth Process. Figure 8 is the energy release rate versus time curve of the original crack growth. In the experimental phenomenon analysis, when $t = 170\,\mu s$, the crack has started to grow. At this moment, the dynamic energy release rate is approximately equal to 2890 N/m, indicating that energy released by the system during the crack growth is enough to provide the energy required for crack growth. From 160 μs to 180 μs, the energy release rate increases at a faster rate. During this time, the arc wave gradually approaches the growing crack. During the period of 190 μs to 240 μs, the energy release rate ranges around the peak value. Subsequently, the energy release rate gradually decays to zero. The above phenomena confirm again that the arc wave has an important influence on the crack growth. In addition, the energy release rate versus time curve is similar to the velocity curve of crack growth.

3.4. Macroscopic and Microscopic Analysis of Crack Growth Process. The experimental study indicates that the growth of the original crack is the result of the combined action of the stress wave and the explosive gas. The stress wave acts on the surrounding rock of the tunnel before the quasi-static stress

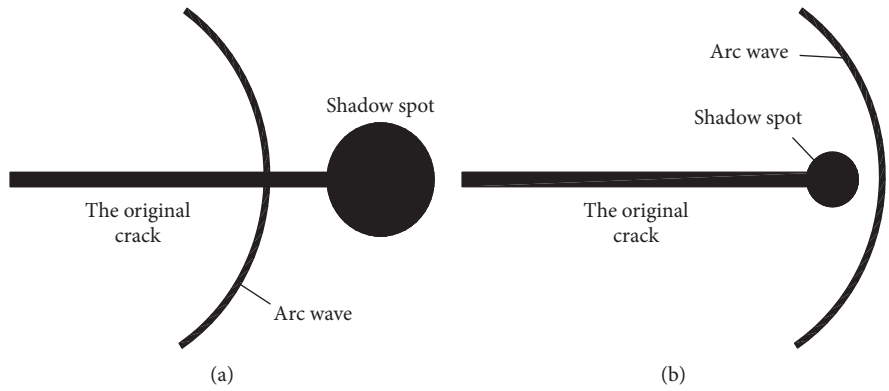

Figure 6: Macroscopic sketch diagram of the crack growth. (a) Macroscopic characteristic of the crack growth process. (b) Macroscopic characteristics of the crack arrest.

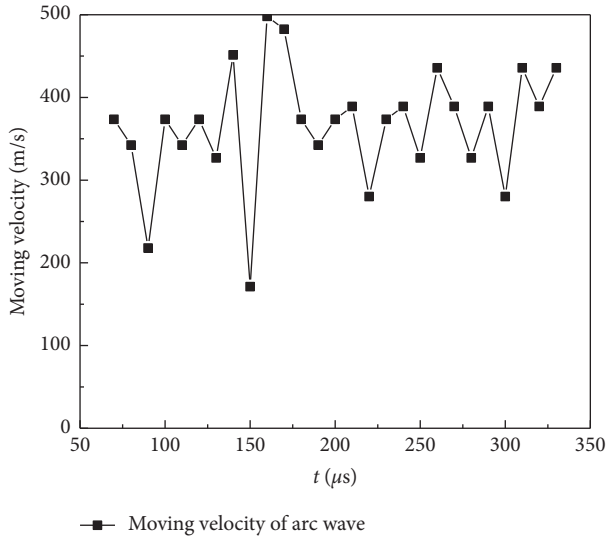

Figure 7: Arc wave velocity curve.

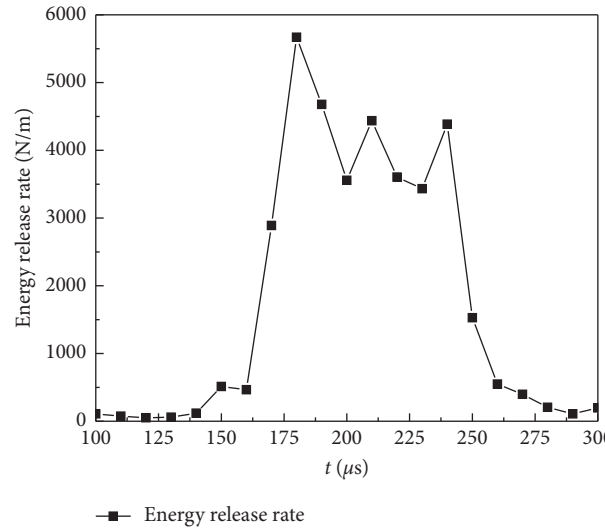

Figure 8: Energy release rate.

of the explosive gas. In addition, the focal speckle diameter at the original crack tip fluctuates, indicating a period of damage evolution before the macroscopic growth of the original crack.

Under the action of stress wave, the microcracks in the surrounding rock of the tunnel are induced or activated. Because the stress wave continuously attenuates during the propagation process, the farther the distance from the explosion source, the smaller the distribution density of microcracks in the surrounding rock. Before the stress wave, the original microcracks in the rock are disordered. Under the action of the stress wave, due to the regularity of the stress field distribution, the activated or induced microcracks have a special distribution law, affecting the growth direction of the original crack.

Under the action of stress wave, the stress of the original crack tip is highly concentrated because of geometrical mutation. More microcracks are activated or induced in a certain direction of the crack tip, causing nonlinear damage, accompanied by the connection of microcracks along the direction, resulting in the formation of a localized damage zone starting from the original crack tip. Since the growth rate of the original crack is significantly smaller than the propagation velocity of the stress wave, according to the weakest chain theory [18], the growth of the macroscopic crack is controlled by the weakest part of the material. Under the action of the stress wave, taking the original crack tip as the starting point, the damage constantly evolves and migrates antecedent to the macroscopic growth of the original crack. The evolution of the damage can be regarded as the connection process between the damage localized zone and the microcrack in a certain direction, forming the damage evolution zone, i.e., the weakest chain. The special distribution law of microcracks in the surrounding rock will affect the migration direction of damage evolution. Due to the action of the same stress field, the migration direction of the damage evolution is consistent with the tendency of activation or induction of microcracks in the surrounding rock mass. Figure 9 shows the growth of the original crack and its penetration with microcracks. Above analysis also verifies the phenomenon that when running cracks propagate near to defects, the crack path deflects toward the defect [19, 20].

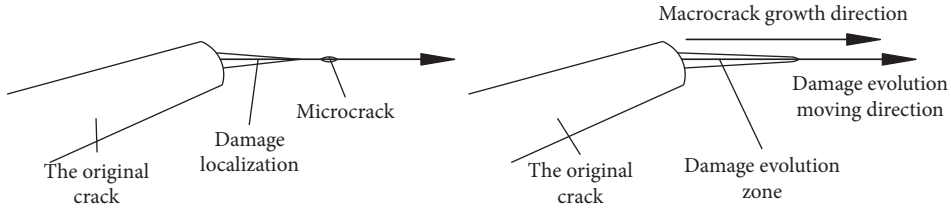

Figure 9: Growth of the original crack and its penetration with microcracks.

The direction of damage evolution determines the direction of macroscopic crack growth, and the accumulation of macrocrack tip energy provides energy for the evolution of damage. When microdamage accumulates to a certain degree, macrocrack can be induced. The high stress concentration at the growing crack tip is the key factor leading the microdamage to the macrocrack. At last, the original crack starts to grow macroscopically along the damage evolution zone.

Since the quasi-static stress generated by the explosive gas lags the stress wave, the quasi-static stress mainly shows as the superposition with the weaken stress field under the action of the stress wave and jointly promotes the growth of the original crack. The effect of quasi-static stress is also time-sensitive. During its action, a new stress peak is formed by superposition with the gradually weakening stress field, i.e., the arc wave is involved in the original crack growth on the back-blasting side. As the arc wave is close to the growing crack, the crack growth rate gradually increases. After the arc wave crosses the propagating original crack, the power source disappears, and the crack growth rate gradually decreases. In addition, away from the blasting source, the activated microcrack distribution density gradually decreases and spacing between microcracks increases. Therefore, the growth resistance of the original crack also gradually increases, and the crack growth kinetic energy decreases, eventually leading to crack arrest. In the late stage of the crack growth, due to the action of unloading wave, the final growth direction of the original crack warps downward.

4. Conclusions

The growth of the original crack in the surrounding rock of the adjacent tunnel results from the combined action of explosion stress wave and explosive gas.

This experimental study indicates that the stress wave and the explosive gas generated by the explosion load are the main factors driving the crack growth. The quasi-static stress generated by the release of the explosive gas acts on the surrounding rock in the form of a pulse wave and is superimposed to the weaken stress wave, forming the main stress difference peak.

The main stress difference peak affects the growth of the original crack in the form of an arc wave. As the arc wave moves close to the growing crack, the crack growth rate gradually increases. When the arc wave passes the crack tip, the crack growth rate significantly weakens. During the period of 200 μs to 250 μs, the crack growth rate oscillates at the peak, and its size is approximately equal to the moving speed of the arc wave. The energy release rate versus time curve is similar to the velocity curve of crack growth.

Based on microscopic damage mechanics, a continuous damage zone is formed near the macrocrack tip. Under the action of explosive load, the damage will be localized in a certain direction. When the micro-cracks runs through the damage localized zone with a certain distribution, the damage evolution zone is formed. Finally, the macrocrack continues to propagate along this direction.

Data Availability

The experimental data used to support the findings of this study are included within the article.

Conflicts of Interest

The authors declare that they have no conflicts of interest.

Acknowledgments

This study was financially supported by the State Key Project of Research and Development Plan of China (2017YFC0804204) and the National Natural Science Foundation of China (51974315 and 51274204).

References

[1] J. Zhao, Y. X. Zhou, A. M. Hefny et al., "Rock dynamics research related to cavern development for ammunition storage," *Tunnelling and Underground Space Technology*, vol. 14, no. 4, pp. 513–526, 1999.

[2] C. Chow, *Diffraction of Elastic Waves and Dynamic Stress Concentrations*, Crane Russak, New York, NY, USA, 1973.

[3] X. H. Li, Y. Long, C. Ji, X. Zhou, and L. Lu, "Dynamic stress concentration factor for tunnel surrounding rock under blasting seismic waves," *Chinese Journal of Geotechnical Engineering*, vol. 35, no. 3, pp. 578–582, 2013.

[4] P. K. Singh, "Blast vibration damage to underground coal mines from adjacent open-pit blasting," *International Journal of Rock Mechanics and Mining Sciences*, vol. 39, no. 8, pp. 959–973, 2002.

[5] Q. Liang, J. Li, D. Li, and E. Ou, "Effect of blast-induced vibration from new railway tunnel on existing adjacent railway tunnel in Xinjiang, China," *Rock Mechanics and Rock Engineering*, vol. 46, no. 1, pp. 19–39, 2013.

[6] X. Xia, H. B. Li, J. C. Li, B. Liu, and C. Yu, "A case study on rock damage prediction and control method for underground tunnels subjected to adjacent excavation blasting," *Tunnelling and Underground Space Technology*, vol. 35, pp. 1–7, 2013.

[7] J. C. Li, H. B. Li, G. W. Ma, and Y. X. Zhou, "Assessment of underground tunnel stability to adjacent tunnel explosion,"

Tunnelling and Underground Space Technology, vol. 35, no. 35, pp. 227–234, 2013.

[8] Z. Zhu, B. Mohanty, and H. Xie, "Numerical investigation of blasting-induced crack initiation and propagation in rocks," *International Journal of Rock Mechanics and Mining Sciences*, vol. 44, no. 3, pp. 412–424, 2007.

[9] G. D. Ming, L. Kang, H. J. Xian, Y. Renshu, Y. Baosen, and Z. Xiaona, "Experimental study on the effect mechanism of the explosion gas on the precrack in the back-blasting of adjacent tunnel," *Journal of China Coal Society*, vol. 41, no. 1, pp. 265–270, 2016.

[10] K. Arakawa, T. Mada, and K. Takahashi, "Correlations among dynamic stress intensity factor, crack velocity and acceleration in brittle fracture," *International Journal of Fracture*, vol. 105, no. 4, pp. 311–320, 2000.

[11] P. S. Theocaris and G. A. Papadopoulos, "The dynamic behaviour of an oblique edge-crack under impact loading," *Journal of the Mechanics and Physics of Solids*, vol. 32, no. 4, pp. 281–300, 1984.

[12] P. S. Theocaris and G. A. Papadopoulos, "The dynamic behaviour of sharp V-notches under impact loading," *International Journal of Solids and Structures*, vol. 23, no. 12, pp. 1581–1600, 1987.

[13] D. Guo, K. Liu, R. Yang, J. Zuo, and J. Fan, "Experimental research on the influence of blasting on the inclined crack in the back-blasting side of nearby roadway," *Journal of Mining and Safety Engineering*, vol. 32, no. 1, pp. 99–104, 2015.

[14] R. S. Yang, Y. B. Wang, and D. M. Guo, "Experimental research of crack propagation in polymethyl methacrylate material containing flaws under explosive stress waves," *Journal of Testing and Evaluation*, vol. 44, no. 1, pp. 248–257, 2016.

[15] G. A. Papadopoulos, "Dynamic caustics and its applications," *Optics and Lasers in Engineering*, vol. 13, no. 3-4, pp. 211–249, 1990.

[16] L. B. Freund, *Dynamic Fracture Mechanics*, Cambridge University Press, Edinburgh, Scotland, 1990.

[17] G. Dongming, Z. Baowei, L. Kang, Y. Renshu, and Y. Pengyang, "Dynamic caustics test of blast load impact on neighboring different cross-section roadways," *International Journal of Mining Science and Technology*, vol. 26, no. 5, pp. 803–808, 2016.

[18] W. Weibull, *A Statistical Theory of the Strength of Materials*, Generalstabens Litografiska Anstalts Förlag, Stockholm, Sweden, 1939.

[19] R. S. Yang, C. X. Ding, L. Y. Yang, P. Xu, and C. Chen, "Hole defects affect the dynamic fracture behavior of nearby running cracks," *Shock and Vibration*, vol. 2018, Article ID 5894356, 8 pages, 2018.

[20] Y. Wang, R. Yang, and G. Zhao, "Influence of empty hole on crack running in pmma plate under dynamic loading," *Polymer Testing*, vol. 58, pp. 70–85, 2017.